Saudi Journal of Biological Sciences 25 (2018) 849–857

Contents lists available at ScienceDirect

Saudi Journal of Biological Sciences

journal homepage: www.sciencedirect.com

Original article

Irisin protects macrophages from oxidized low density lipoprotein-induced apoptosis by inhibiting the endoplasmic reticulum stress pathway

Guanlin Zheng [a,b], Haizhen Li [a,c], Tie Zhang [d], Libo Yang [d], Shutong Yao [e], Shihong Chen [a,*], Maochuan Zheng [f], Qin Zhao [g], Hua Tian [e]

[a] Department of Endocrinology and Metabolism, Second Hospital of Shandong University, Ji'nan, Shandong Province, China
[b] Taishan Vocational College of Nursing, Taian, Shandong Province, China
[c] Department of Endocrinology, Dongying City District People Hospital, Dongying, Shandong Province, China
[d] Department of Endocrinology, Taian City Central Hospital, Taian, Shandong Province, China
[e] Key Laboratory of Atherosclerosis in Universities of Shandong and Institute of Atherosclerosis, Taishan Medical University, Taian, Shandong Province, China
[f] Graduate School of Taishan Medical University, Taian, Shandong Province, China
[g] Department 2 of Gastroenterology, Taian City Central Hospital, Taian, Shandong Province, China

ARTICLE INFO

Article history:
Received 11 August 2017
Revised 24 August 2017
Accepted 26 August 2017
Available online 30 August 2017

Keywords:
Irisin
Endoplasmic reticulum stress
Macrophage
Apoptosis

ABSTRACT

Irisin is a newly discovered myokine which can relieve metabolic disorders and resist atherosclerosis. The effects of irisin on ox-LDL-induced macrophage apoptosis and endoplasmic reticulum stress-related pathways were observed *in vitro*. RAW264.7 macrophages were cultured *in vitro* and pretreated with irisin at 20, 40 and 80 ng/ml for 30 min, followed by culture with 100 mg/L ox-LDL and 5 mg/L tunicamycin (TM) for 12 h. The cell viability and apoptosis were detected by MTT assay and annexin V-FITC double staining. The nuclear translocation of activating transcription factor 6 (ATF6) was detected by immunofluorescence assay. Western blot was used to detect the expressions of p-PERK, p-eIF2α, C/EBP homologous protein (CHOP) and Bcl-2. Irisin reduced lipid accumulation in macrophages in a concentration-dependent pattern and significantly inhibited apoptosis induced by ox-LDL and TM. Compared with ox-LDL and TM groups, the expressions of CHOP, p-PERK and p-eIF2α in the irisin group significantly decreased, the translocation of ATF6 from cytoplasm to nucleus was significantly weakened, and Bcl-2 expression significantly increased. Irisin can alleviate the apoptosis of macrophages induced by ox-LDL, which may be achieved by inhibiting the PERK/eIF2α/CHOP and ATF6/CHOP endoplasmic reticulum stress signaling pathways.

1. Introduction

Atherosclerosis is characterized by the formation of lipid-rich atherosclerotic plaques in the vessel wall. The deposition of lipoprotein rich in apolipoprotein E to the vessel wall leads to endothelial cell dysfunction which causes the adhesion and migration of mononuclear cells to subcutaneous tissues. Mononuclear cells differentiate into macrophages which can phagocytose oxidized low density lipoprotein (ox-LDL) to form foam cells. The accumulation of ox-LDL in macrophages and oxidative stress can promote the apoptosis of macrophages and increase the fragility of plaques. The thrombosis caused by fragile plaque rupture is mainly responsible for acute cardiovascular events (Finn et al., 2010).

Endoplasmic reticulum stress (ERS) is an important pathway for macrophage apoptosis induced by ox-LDL (Scull and Tabas, 2011). Excessive or prolonged ERS can activate unfold protein response (UPR). Protein kinase RNA-like ER kinase (PERK), inositol requiring protein 1α (IRE1 α) and activating transcription factor 6 (ATF6) are considered to be three branched channels involved in UPR initiation. The activation of PERK and ATF6 can induce the expression of CHOP (C/EBP homologous protein), and IRE1 α can activate c-Jun amino-terminal kinase (JNK). Both JNK and CHOP can inhibit the expression of anti-apoptotic factor Bcl-2 and activate the

* Corresponding author.
E-mail address: chenshshsu@foxmail.com (S. Chen).
Peer review under responsibility of King Saud University.

Production and hosting by Elsevier

http://dx.doi.org/10.1016/j.sjbs.2017.08.018
1319-562X/

calcium signaling pathway, causing macrophage apoptosis (Tabas and Ron, 2011).

Irisin is a hormone that is mainly secreted by muscle cells, which was reported for the first time in 2012 (Bostrom et al., 2012). It can increase energy consumption by promoting white fat browning, and relieve a variety of metabolic disorders, including obesity, insulin resistance, hyperglycemia and hyperlipidemia (Bostrom et al., 2012; Zhang et al., 2014; Xiong et al., 2015). Further *in vitro* and animal studies have demonstrated that irisin may have direct therapeutic effects on atherosclerosis. It can also inhibit high glucose-induced endothelial cell apoptosis, promote endothelial cell proliferation, and alleviate endothelial cell dysfunction (Song et al., 2014; Fu et al., 2016a; Zhang et al., 2016; Zhu et al., 2016). Lu et al. (2015) found using a model of diabetic mice with apolipoprotein E knockout that irisin treatment reduced the atherosclerotic plaque area, inflammatory cell infiltration on the vascular wall and inflammatory factor expression. In humans, irisin has been found in the paraventricular hypothalamic nucleus and cerebrospinal fluid, but its role in the central nervous system remains unclear, probably participating in the differentiation of neurons and motor coordination (Dun et al., 2013). Injecting the third ventricle of rats with recombinant irisin can activate neurons in the paraventricular hypothalamic nucleus, thereby elevating blood pressure and enhancing myocardial contraction (Wrann et al., 2013). Injecting irisin into the central nervous system also increases the activity and oxygen consumption of rats (Zhang et al., 2015).

However, the effects of irisin on macrophage apoptosis or ERS have never been evaluated hitherto. Therefore, this study aimed to explore the therapeutic effects of irisin on atherosclerosis by investigating the influence of irisin on ox-LDL-induced macrophage apoptosis, ERS and ERS-related signaling pathways.

2. Materials and methods

2.1. Materials

Mouse RAW264.7 macrophages were purchased from Shanghai Institute of Biochemistry and Cell Biology (China). Irisin was bought from Phoenix Pharmaceuticals (USA). MTT, oil red O, tunicamycin (TM) and rabbit anti-β-actin monoclonal antibody were obtained from Sigma (USA). Rabbit antibodies against CHOP, Bcl-2, p-PERK and p-eIF2α were provided by Santa Cruz (USA). Rabbit anti-ATF6 polyclonal antibody was purchased from Abcam (USA). Goat anti-rabbit IgG and ready-to-use SABC-Cy3 immunohistochemical kit were bought from Beijing Zhong Shan-Golden Bridge Biological Technology Co., Ltd. (China) and Wuhan Boster Biological Technology Co., Ltd. (China) respectively. DMEM high-glucose culture medium and fetal bovine serum were provided by Gibco (USA). RIPA lysis solution and BCA protein quantification kit were purchased from Solarbio (USA). Annexin V-FITC apoptosis detection kit was bought from Nanjing Keygen Biotech. Co., Ltd. (China). Trizol reagent was obtained from Invitrogen (USA). cDNA synthesis kit and Real Master Mix (SYBR Green) kit were provided by Tiangen Biotech (Beijing) Co., Ltd. (China). ECL kit and PVDF membrane were purchased from Pierce (USA) and Millpore (USA) respectively. Other reagents were all analytically pure.

2.2. LDL separation and oxidation

Ox-LDL was prepared according to the method described previously (Yao et al., 2013). First, fresh human plasma LDL was isolated by serial ultracentrifugation, dialyzed with PBS without EDTA for 48 h, then incubated in PBS containing 10 μmol/L $CuSO_4$ (pH 7.2) at 37 °C for subsequent 18 h of dialysis, and finally dialyzed in PBS containing 100 μmol/L EDTA at 4 °C for 24 h. After sterile filtration, the protein was quantified using BCA reagent, and the protein concentration was adjusted to 1 g/L with PBS and stored at 4 °C. The concentration of the thiobarbituric acid reactive substance of MDA was measured (>30 μmol/g). Agarose gel electrophoresis showed that the electrophoretic mobility of ox-LDL was increased 2- to 2.5-fold that of LDL.

2.3. Cell culture and experimental grouping

RAW264.7 macrophages with normal growth were cultured in DMEM high glucose medium (containing 10% fetal bovine serum, penicillin 100 U/mL, streptomycin 100 μg/mL) to a cell density of 1×10^8 cells/L, and placed in a 5% CO_2 incubator at 37 °C. The cells were transferred to DMEM containing 0.1% fetal bovine serum 24 h before treatment.

Experimental grouping (1): They were randomly divided into a control group: routinely cultured in the culture medium; an ox-LDL group: 100 mg/L ox-LDL was added to the culture medium; and irisin intervention groups: irisin (20, 40 and 80 ng/ml) was added to the culture medium for pretreatment for 30 min, followed by 100 mg/L ox-LDL. Except the irisin pretreatment group, other groups were added with dimethyl sulfoxide (DMSO) with volume fraction of 0.1%, and cultured for 24 h.

Experimental grouping (2): They were divided into a control group: DMSO with volume fraction of 0.1% for conventional culture; a TM group: the culture medium was added with 5 mg/L TM; and an irisin intervention group: 80 ng/ml irisin was added to the culture medium for pretreatment for 30 min, followed by 5 mg/L TM. The cells were collected 12 h after treatment.

2.4. Observation of intracellular lipid droplet changes by oil red O staining

The cells were seeded in 6-well culture plates (built-in sterile cover slips). After treatment, the cells were rinsed with PBS, fixed with 4% calcium formaldehyde solution, stained with oil red O for 15 min, counterstained with hematoxylin for 3 min, and then observed under Olympus BX51 microscope. Intracellular lipid was red and the nucleus was blue. Five fields were randomly selected for each cover slip, and the results were analyzed by Image-Pro Plus 6.0 (Media Cybernetics) software. The cell mean integrated absorbance (IA) was used to express the content of intracellular lipid droplet. The experiment was repeated three times, two repeated wells for each group each time (Yao et al., 2013).

2.5. Detection of cell viability by MTT assay

The cells with normal growth were cultured in 96-well culture plates at a density of 1×10^4/L. After treatment, the cells were added MTT (final concentration of 0.5 g/L) and continued to be incubated for 4 h in the incubator. The supernatant was discarded, and 200 μL of DMSO was added to each well. The optical density (OD) of each well was measured at 490 nm using the Infinite F200 Multifunctional Microplate Reader (Tecan, Switzerland). With the cell viability of the control group as 100%, the viability of the other groups was expressed as a percentage of OD to that of the control group.

2.6. Detection of cell apoptosis by flow cytometry

The cells of each group were collected, with the density adjusted to 5×10^5/mL at 4 °C, centrifuged at 1000 r/min for 10 min, and then rinsed twice with ice-cold PBS. The supernatant was discarded and the cells were resuspended with 100 μL of binding buffer. Subsequently, 5 μL of annexin V-FITC and 5 μL of

propidium iodide (PI) were added to each well. After incubation, the cells were incubated at room temperature for 15 min, and finally added 400 μL of binding buffer. Cell apoptosis was detected using flow cytometry (Becton-Dickinson, CA, USA). Apoptotic cells were distinguished and quantified into four subsets, including normal living cells (lower left quadrant: annexin-/PI−), necrotic cells (upper left quadrant: annexin-/PI+), early apoptotic cells (lower right quadrant: annexin+/PI−) and advanced apoptotic cells (upper right quadrant: annexin+/PI+). Total apoptotic rate (%) = early apoptotic rate (%) + late apoptotic rate (%).

2.7. Detection of ATF6 nuclear translocation

The cells were seeded in 6-well culture plates with sterile cover slips. After treatment, operations were conducted according to the SABC-Cy3 immunohistochemical kit. The cells were rinsed with PBS 3 times, fixed with 4% paraformaldehyde for 30 min, rinsed again with PBS, then treated with 0.1% Triton-X 100 at room temperature for 10 min, blocked with goat serum, placed in 1:200 diluted rabbit anti-mouse ATF6 primary antibody, incubated overnight at 4 °C, then placed in goat anti-rabbit biotinylated secondary antibody (1:100), incubated at 37 °C for 30 min, dropwise added SABC-Cy3 complex (1:100 dilution), incubated at 37 °C for 30 min, rinsed fully with PBS, and mounted with water-soluble mounting medium. PBS was used to replace primary antibody as a negative control. Positive expression was bright red under the fluorescence microscope (Olympus BX51).

2.8. Western blot

After the cells were treated, total protein was extracted according to the instructions of the RIPA Total Protein Extraction Kit. After denaturation and quantification, the cells were stored at −80 °C before use. Then 8–15% separation gel was prepared for sodium dodecyl sulfate-polyacrylamide gel electrophoresis (sample volume of 40 μg), and the products were electrically transferred to a PVDF membrane. The corresponding membranes of target protein band and internal reference band were cut according to the position of marker. After blocking with 5% skimmed milk, rabbit anti-CHOP (1:400), Bcl-2 (1:400), p-PERK (1:400) and p-eIF2α (1:400) polyclonal antibodies were used for incubation overnight at room temperature. The membranes were washed three times, and incubated in corresponding secondary antibodies labeled with horseradish peroxidase for 2 h. β-Actin antibody (1:8000) was used as the internal reference. Antigen–antibody complex was analyzed by ECL method, and X-ray film was exposed in dark. The integrated optical density (IOD) values of protein bands were analyzed using Image-Pro Plus software (Version 6.0, Media Cybernetics, MD, USA), with the target protein's IOD/internal reference's IOD ratio reflecting the relative level of target protein.

2.9. Statistical analysis

All data were expressed as mean ± SD, and analyzed by SPSS12.0 software for one-way analysis of variance. Means

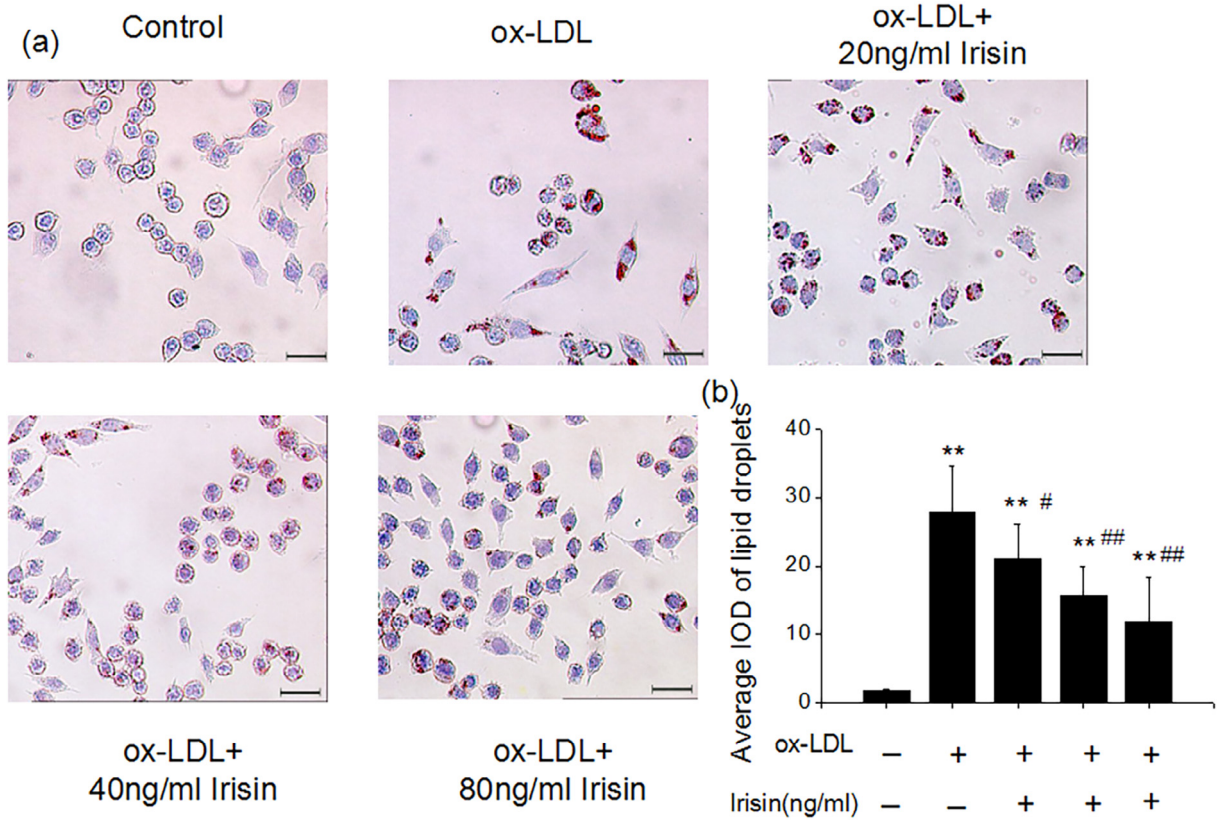

Fig. 1. Irisin reduces ox-LDL-induced intracellular lipid accumulation in RAW264.7 cells. (a) Cells were treated with ox-LDL (100 mg/L) in the absence or presence of irisin at different concentrations (20, 40 and 80 ng/ml) for 24 h, and the intracellular lipid droplets were stained by oil red O. Representative lipid droplet staining images are shown. Scale bar = 20 μm. (b) The average IOD of lipid droplets stained with oil red O from differentiated macrophage foam cells was obtained via checking five fields in each condition. Data are presented as the mean ± SEM of at least four independent experiments. $^{**}P < 0.01$ versus vehicle-treated control; $^{\#}P < 0.05$, $^{\#\#}P < 0.01$ versus ox-LDL treatment. ox-LDL, oxidized LDL.

between two groups were compared by the SNK method. $P < 0.05$ was considered statistically significant.

3. Results

3.1. Irisin inhibited ox-LDL-induced lipid accumulation in RAW264.7 macrophages

After staining with oil red O, the cells with red intracellular lipid were positive. There were fewer or no positive cells in the control group, but positive cells widely existed in the ox-LDL group. The irisin (20, 40 and 80 ng/ml) pretreatment groups had significantly fewer positive cells, with their IOD values accounting for 76.74%, 56.50% and 42.3% of that of the ox-LDL group ($P < 0.01$ for the latter two) (Fig. 1).

3.2. Effects of irisin on survival rates of ox-LDL- and TM-induced RAW264.7 macrophages

MTT assay showed that compared with the control group, there was no significant difference in viability after RAW264.7 cells were treated with 20, 40 and 80 ng/ml irisin for 12 h ($P > 0.05$) (Fig. 2a). However, irisin alleviated the reduction of cell viability induced by ox-LDL (100 mg/L). Compared with the normal group, the cell viability of the ox-LDL group decreased by 47.7%, while compared with the ox-LDL group, the viability of the 20, 40 and 80 ng/ml irisin pretreatment groups increased in a dose-dependent manner (13.0%, 26.9%, and 44.2%, respectively) ($P < 0.05$) (Fig. 2b). With the TM group as a positive control, the results showed that irisin attenuated the reduction of TM-induced RAW264.7 cell survival rate (Fig. 2c).

3.3. Effects of irisin on apoptosis of ox-LDL- and TM-induced RAW264.7 macrophages

Flow cytometry showed that the total apoptosis rate of the ox-LDL group was significantly higher than that of the control group ($P < 0.05$). After the combined action of irisin (20, 40 and 80 ng/ml) and ox-LDL, the total apoptosis rate significantly reduced dose-dependently compared with that of the ox-LDL group ($P < 0.05$) (Fig. 3a).

The TM group was taken as a positive control to observe the effect of irisin on the apoptosis of macrophages. The increased apoptosis rate of macrophages induced by TM was decreased by irisin (Fig. 3b).

3.4. Effects of irisin on CHOP and Bcl-2 protein expressions in ox-LDL- and TM-induced RAW264.7 macrophages

Western blot showed that the level of CHOP protein in the ox-LDL treatment group was significantly higher than that in the control group, and the expression of Bcl-2 protein significantly decreased by 29.9% ($P < 0.01$) compared with the control group ($P < 0.01$). Besides, 20, 40 and 80 ng/ml irisin pretreatment significantly inhibited TM-induced CHOP up-regulation and Bcl-2 down-regulation dose-dependently ($P < 0.05$ or $P < 0.01$) (Fig. 4a).

In the TM-induced intracellular ERS model, the effects of irisin were similar to the above-mentioned ones. Compared with the TM group, the expression of CHOP protein reduced by 22.4% and

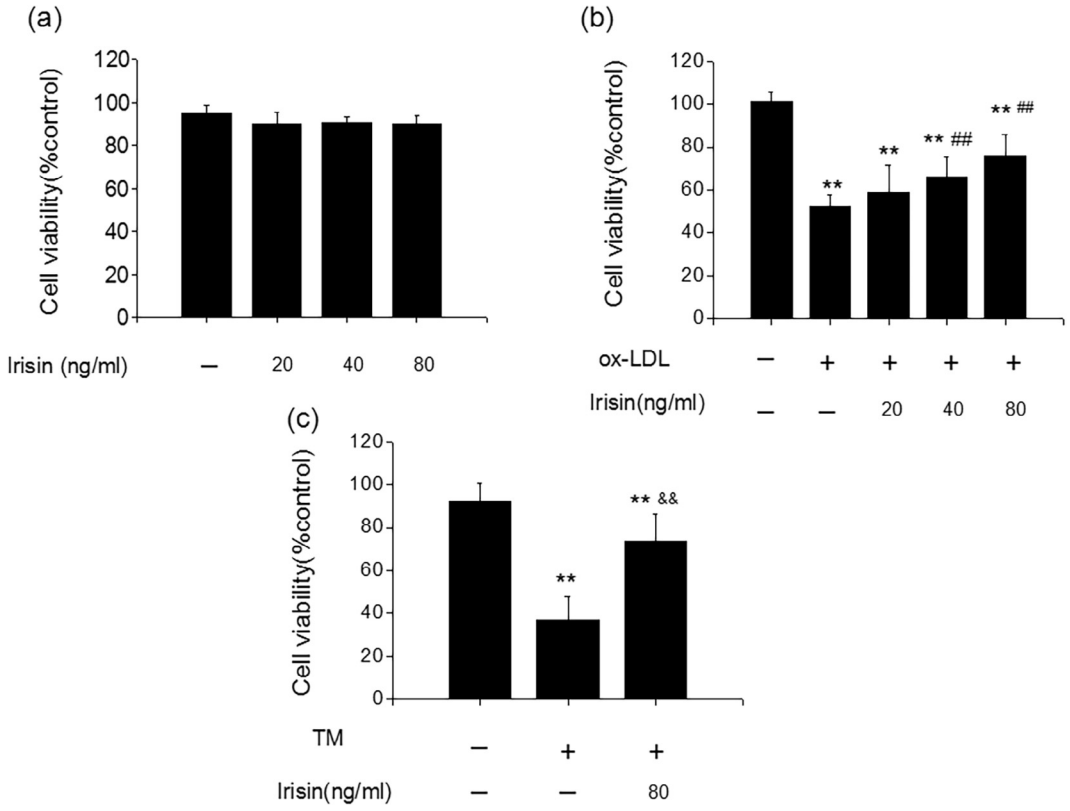

Fig. 2. Effects of irisin on cell viability. (a) Determination of the cytotoxic effects of irisin on RAW264.7 cells. Cells were treated with different concentrations (20, 40 and 80 ng/ml) of irisin for 24 h. (b) Irisin inhibits ox-LDL-induced cell death. Cells were treated with different concentrations (20, 40 and 80 ng/ml) of irisin in the presence of ox-LDL (100 mg/L) treatment for 24 h. (c) Irisin inhibits TM-induced cell death. Cells were treated with irisin (80 mmol/L) in the presence of TM (5 mg/L) for 12 h. The viability of cells under different treatments was measured by MTT assay and expressed as the percentage of control (survival of control). Data are expressed as the mean ± SEM of at least three independent experiments. $^{**}P < 0.01$ versus vehicle-treated control; $^{\#\#}P < 0.01$ versus ox-LDL treatment; $^{\&\&}P < 0.01$ versus TM treatment. ox-LDL, oxidized LDL.

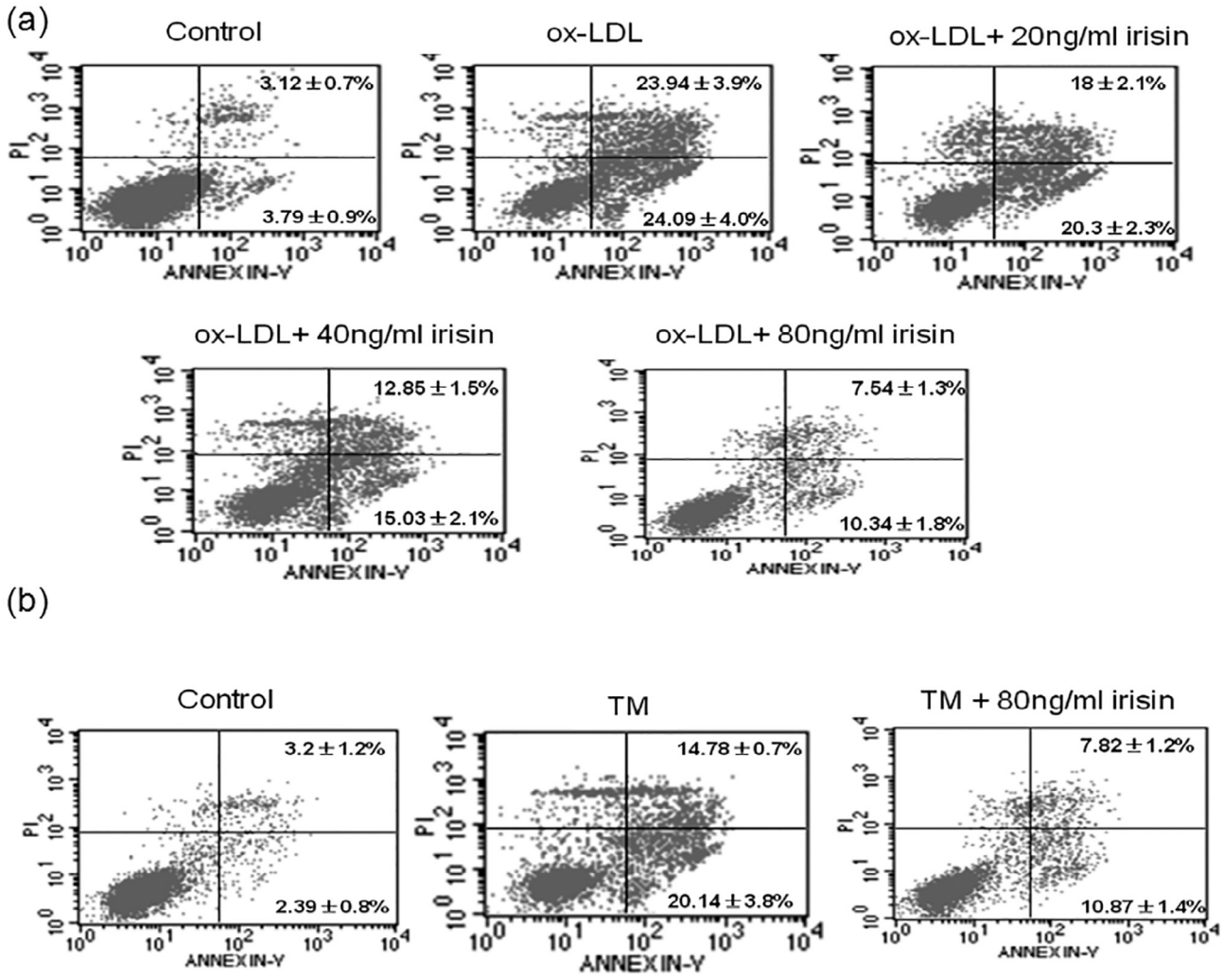

Fig. 3. Irisin decreases apoptosis induced by ox-LDL or TM in RAW264.7 cells. (a) Cells were treated with ox-LDL (100 mg/L) in the absence or presence of irisin at different concentrations (20, 40 and 80 ng/ml) for 24 h, and the population of apoptotic cells stained with Annexin V-FITC and PI was detected by flow cytometry analysis. (b) Cells were treated with TM (5 mg/L) in the absence or presence of irisin (80 ng/ml) for 12 h, and the ratio of apoptotic cells stained with Annexin V-FITC and PI was detected by flow cytometry analysis. A representative of data of flow cytometry analysis was presented. The percentage of apoptotic cells under different treatments was measured and expressed as the mean ± SEM from three independent experiments. ox-LDL, oxidized LDL; PI, propidium iodide.

the expression of Bcl-2 protein increased by 147% in the 80 nmol/L irisin pretreatment group (Fig. 4b).

3.5. Irisin inhibited ATF6 nuclear translocation in ox-LDL-induced macrophages

Intracellular ATF6 was shown by SABC-Cy3 immunofluorescence assay (Fig. 5), with the red fluorescence area as positive expression. The red fluorescence of the control group was mainly located in the cytoplasm, but little or none in the nucleus. There was strong fluorescence staining in the nucleus of the ox-LDL group. Compared with the ox-LDL group, the red fluorescence intensity of the irisin pretreatment group was weakened with rising irisin concentration in the nucleus of the irisin pretreatment group.

3.6. Effects of irisin on p-PERK and p-eIF2α protein expressions in ox-LDL-induced macrophages

Western blot showed that the levels of p-PERK and p-eIF2α proteins in the ox-LDL treatment group increased 1.93-fold and 1.98-fold respectively compared with those of the control group ($P < 0.01$). After 20, 40 and 80 ng/ml irisin pretreatment, the up-regulation of p-PERK and p-eIF2α induced by TM was inhibited in a concentration-dependent manner ($P < 0.05$ or $P < 0.01$) (Fig. 6).

4. Discussion

In vitro study was conducted to first observe the effects of different concentrations of irisin on lipid accumulation in macrophages and the effects of ox-LDL and TM (ERS inducer) on apoptosis. Irisin inhibited lipid deposition in macrophages in a concentration-dependent manner, and reduced ox-LDL- and TM-induced macrophage apoptosis by suppressing ERS-related signaling pathways.

Unstable plaque rupture and thrombosis are the main causes of acute cardiovascular events (Finn et al., 2010) Macrophage infiltration, fibrous cap thinning and necrotic center expansion are the characteristics of unstable plaques, and macrophage apoptosis and the resulting necrotic center expansion are one of the important mechanisms of unstable plaque occurrence (Otsuka et al., 2016). Therefore, inhibition of macrophage apoptosis may be one of the treatment measures for stable plaque. Irisin, as a newly discovered myokine, is mainly synthesized and secreted by skeletal muscle cells. A number of studies have confirmed that irisin

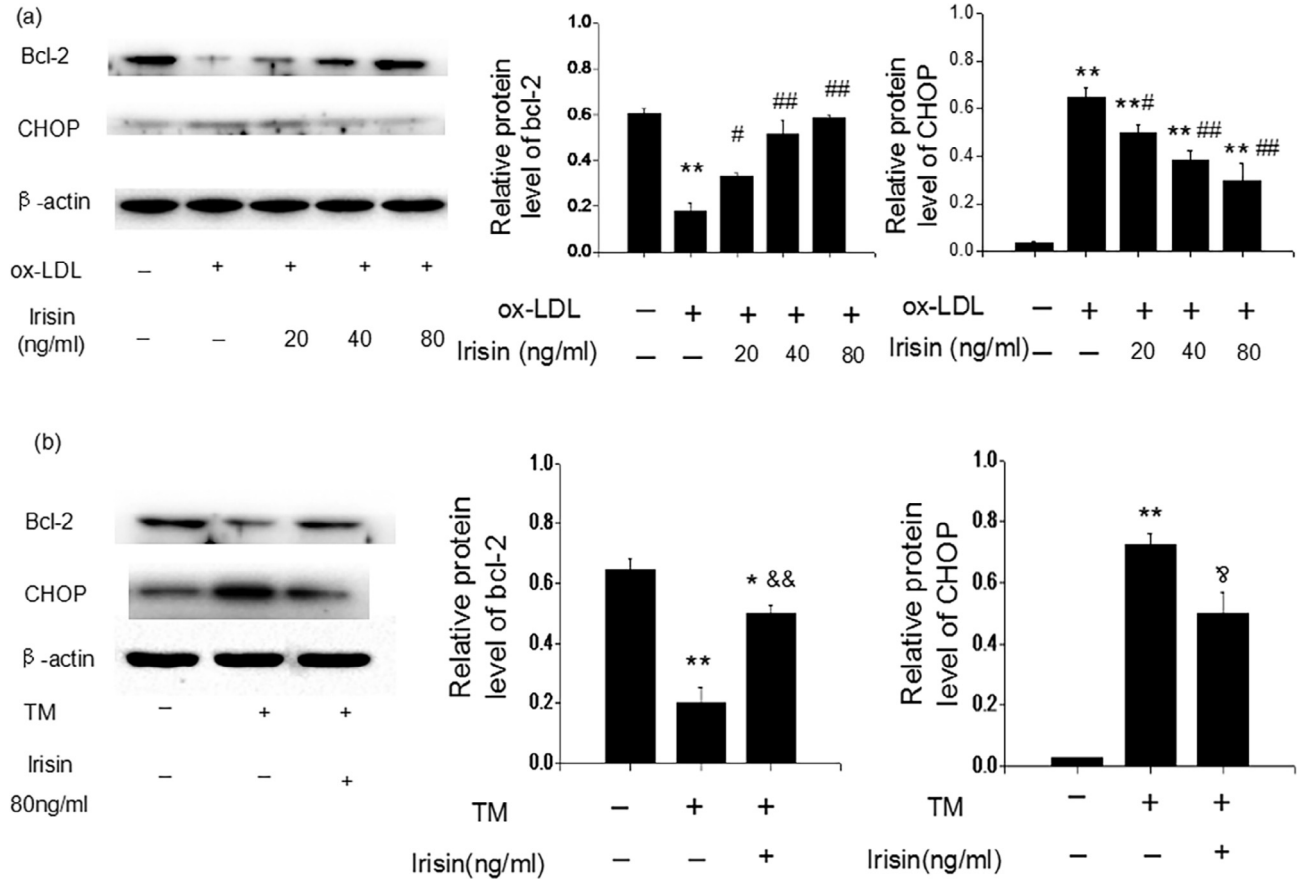

Fig. 4. Effect of irisin on CHOP and Bcl-2 expression induced by ox-LDL or TM in RAW264.7 cells. Cells were treated as described in Fig. 3. The expression of CHOP and Bcl-2 were analyzed by Western blot and normalized to β-actin levels (a and b). Data are presented as the mean ± SEM of at least three independent experiments. $^{*}P < 0.05$, $^{**}P < 0.01$ versus vehicle-treated control; $^{\#}P < 0.05$, $^{\#\#}P < 0.01$ versus ox-LDL treatment; $^{\&}P < 0.05$, $^{\&\&}P < 0.01$ versus TM treatment. ox-LDL, oxidized LDL; CHOP, C/EBP homologous protein.

mitigates various metabolic disorders, including insulin resistance (Bostrom et al., 2012; Zhang et al., 2014; Xiong et al., 2015). As the occurrence of atherosclerosis is closely related to insulin resistance and other metabolic diseases, the therapeutic effects of irisin on atherosclerosis have attracted much attention. Studies have shown that irisin can protect against high glucose- and ox-LDL-induced endothelial cell dysfunction, inhibit vascular inflammation and plaque progression, and reduce blood pressure (Lu et al., 2015; Fu et al., 2016a,b; Zhang et al., 2016). In this study, we assessed the therapeutic effects of irisin on the atherosclerosis of macrophages. *In vitro* cell studies showed that irisin reduced lipid accumulation in macrophages in a dose-dependent manner, inhibited ox-LDL-induced macrophage apoptosis, and promoted cell survival. Irisin may stabilize plaques by inhibiting the transformation of macrophages into foam cells and macrophage apoptosis. The above inferences need to be confirmed *in vivo*. In arteriosclerotic mice with apolipoprotein E knockout, exercises can stabilize plaques by reducing macrophage infiltration, oxidative stress, inflammatory factors and matrix metalloproteinase expression (Shimada et al., 2011; Kadoglou et al., 2013). As exercises can enhance the synthesis of irisin, it mediates the effect of exercises on the alleviation of obesity and other metabolic disorders, but whether irisin stabilizes plaques by exercises needs to be further studied. There have been no other studies reporting the influence of irisin on macrophage apoptosis. *In vitro* studies of Bosma et al. (2016) showed that FNDC4 bound closely to bone marrow-derived macrophages, attenuatd their phagocytosis, increased cell viability, and reduced macrophage expression of proinflammatory cytokines. FNDC4 is highly homologous to irisin precursor-FNDC5 and belongs to the fibronectin type III domain family of proteins (Teufel et al., 2002), suggesting that irisin can inhibit macrophage apoptosis.

The endoplasmic reticulum is an organelle that exists in all eukaryotic cells, with the ability to accurately fold secreted proteins. Ox-LDL and other stress factors can interfere with the protein folding process of the endoplasmic reticulum, resulting in the accumulation of unfolded and misfolded proteins, which is a process known as ERS (Feng et al., 2003). The endoplasmic reticulum deals with ERS by activating multiple intracellular signaling pathways which are collectively referred to as UPR (Tabas, 2010). When UPR cannot maintain the steady state of endoplasmic reticulum, the apoptotic signaling pathway is activated to cause apoptosis. ERS is an important mechanism of ox-LDL-induced macrophage apoptosis. In this study, irisin inhibited both ox-LDL- and TM-induced macrophage apoptosis. As TM is a classic ERS inducer, irisin may exert the anti-apoptotic effect by inhibiting ERS. It has been confirmed that CHOP, as an important effector of ERS-mediated apoptosis, can promote apoptosis by down-regulating the expression of anti-apoptotic molecule Bcl-2 and activating calcium signaling pathways (Rutkowski et al., 2006). In addition, *in vitro* and *in vivo* studies have confirmed that CHOP gene knockout can inhibit macrophage apoptosis, and reduce plaque necrosis and rupture (Thorp et al., 2009; Tsukano et al., 2010), suggesting that CHOP is closely associated with macrophage apoptosis, plaque progression and rupture. Therefore, this study further evaluated the effect of irisin on CHOP expression. Irisin significantly inhibited ox-LDL- and TM-induced expression of CHOP in a concentration-dependent pattern, and up-regulated the expression of Bcl-2, suggesting that irisin resisted macrophage apoptosis partially by

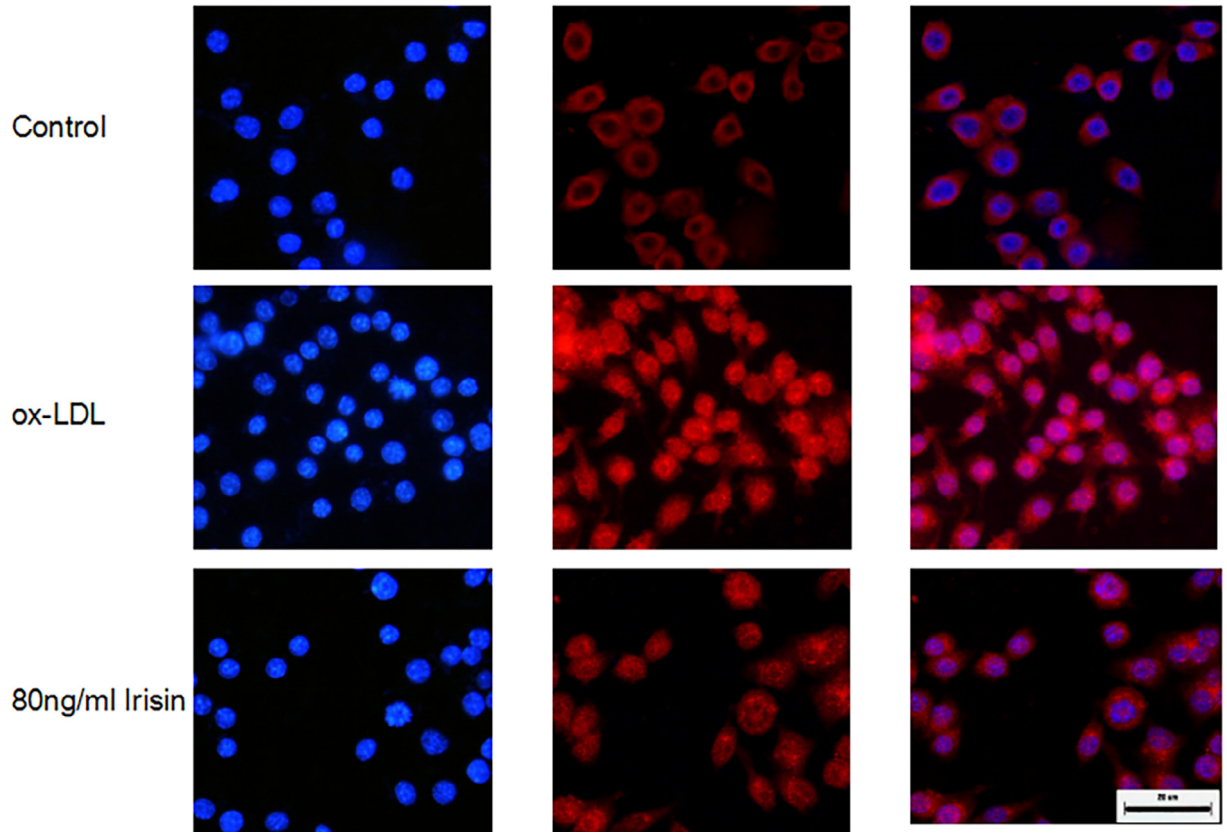

Fig. 5. Irisin inhibits nuclear translocation of ATF6 in RAW264.7 macrophages. Cells were treated as described in Fig. 3. Immunofluorescence experiments show ATF6 visualized by Cy3 labeling (red) and nuclei stained with DAPI (blue) with laser scanning confocal microscope. Representative fluorescent images are shown. Scale bar = 20 μm. DAPI, 4′,6-diamidino-2-phenylindole; ATF6, activating transcription factor 6; ox-LDL, oxidized LDL.

inhibiting CHOP expression. Song et al. (2014) reported that irisin inhibited endothelial cell apoptosis via the ERK signaling pathway. Whether the pathway is involved in the regulation of macrophage apoptosis by irisin needs further studies. Wang et al. (2017) found that irisin improved the mitochondrial function by reducing the mitochondrial permeability transition pore opening and mitigating mitochondrial edema, thus protecting cardiomyocytes from ischemia-reperfusion injury. Since both mitochondria- and non-mitochondrial-dependent pathways are involved in CHOP-induced macrophage apoptosis (Scull and Tabas, 2011), whether mitochondria are involved in the effect of irisin on macrophage apoptosis needs to be confirmed by further studies.

PERK and ATF6 are upstream regulators of CHOP. The misfolded protein under ERS can lead to PERK phosphorylation with endoplasmic reticulum combination and activation of ATF6. Phosphorylated PERK can phosphorylate the α subunit of eIF2α, then the phosphorylated eIF2α can activate the activating transcription factor 4 (ATF4), and then up-regulate CHOP expression (Ron and Walter, 2007). After being activated, ATF6 is shorn by protein kinases SP1 and SP2 located in the Golgi apparatus, and then translocated to the nucleus, thereby up-regulating the expressions of a variety of genes involved in protein folding and degradation, including CHOP and NF-κB (Yamazaki et al., 2009). Therefore, this study further assessed the effect of irisin on the expression of phosphorylated PERK/eIF2α and the nuclear translocation of ATF6. Irisin significantly inhibited the expressions of phosphorylated PERK and eIF2α induced by ox-LDL and TM, and reduced the nuclear translocation of ATF6 in a concentration-dependent pattern, indicating that irisin alleviated ox-LDL-induced macrophage apoptosis via PERK/eIF2α/CHOP/Bcl-2 and ATF6/CHOPERS signaling pathways. Irisin-specific receptors and the specific signaling pathways that interact with different cells have not been clarified yet, so the specific mechanisms of irisin for PERK phosphorylation and ATF6 nuclear translocation need to be further studied.

We found that irisin inhibited ox-LDL uptake by macrophages. Wintergerst et al. (2000) reported that CD36 mediated ox-LDL uptake by macrophages and ox-LDL-induced ERS. Whether irisin suppresses such uptake and the ERS-CHOP pathway by down-regulating CD36 still needs further studies.

Regardless, this study has the following limitations. (1) This study did not observe the specific mechanism of irisin for reducing lipid accumulation in macrophages, such as the effect of irisin on the expressions of scavenger receptors in macrophages. (2) The currently known three UPR branches were PERK, ATF6 and IRE1. The effect of irisin expression was not observed. (3) Although irisin may inhibit ox-LDL- and TM-induced macrophage apoptosis via the CHOP signaling pathway, this postulation and the effect of the signaling pathway on the anti-apoptotic effect of irisin need to be confirmed by knockout of CHOP gene.

In conclusion, we reported, for the first time, that irisin reduced lipid accumulation in macrophages *in vitro* and inhibited ox-LDL- and TM-induced macrophage apoptosis by PERK/eIF2α/CHOP/Bcl-2 and ATF6 ERS, suggesting that irisin may have therapeutic effects on the progress and stability of atherosclerotic plaques. The findings of this study need to be further confirmed by *in vivo* studies.

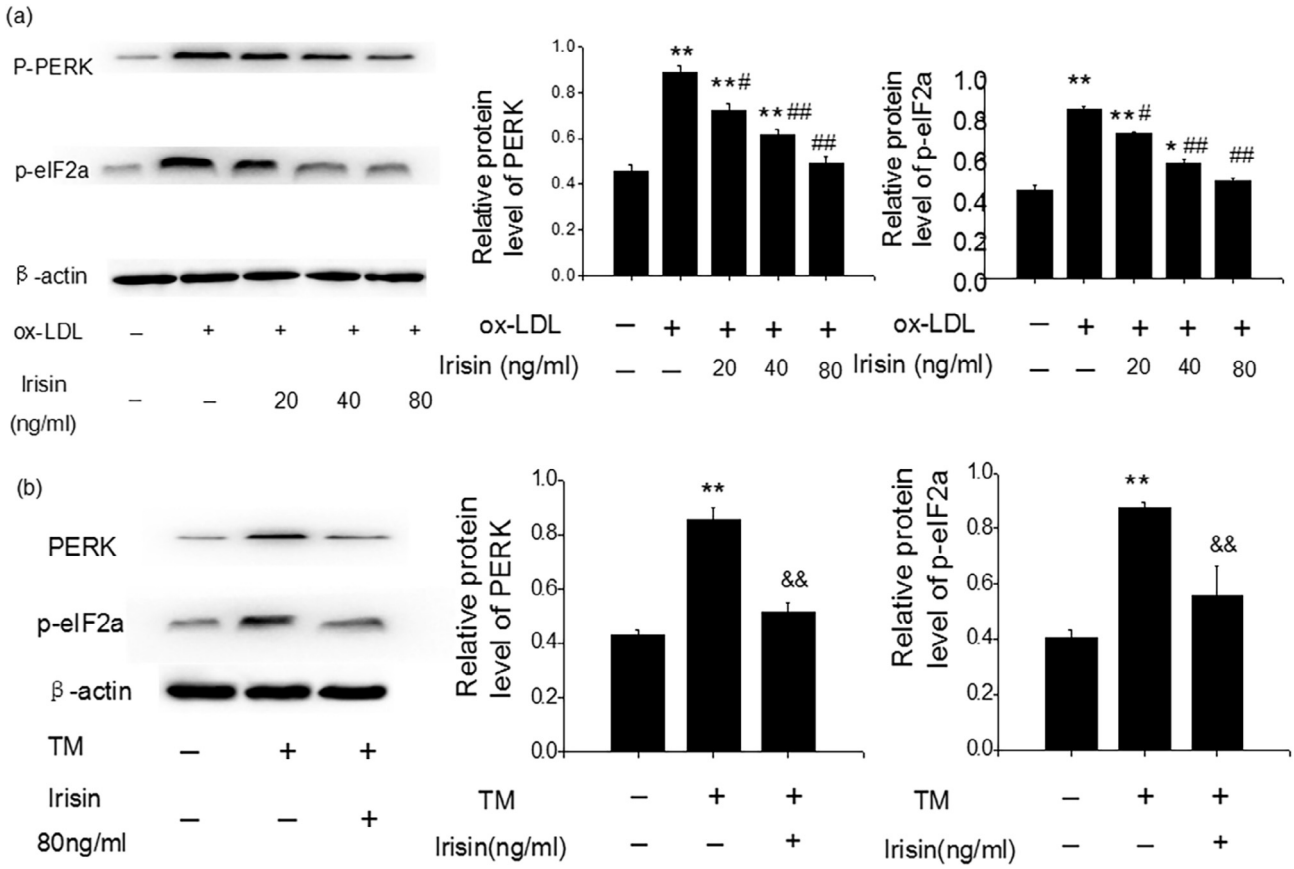

Fig. 6. Irisin inhibits the upregulation of p-PERK and p-eIF2α expression induced by ox-LDL or TM in RAW264.7 cells. Cells were treated as described in Fig. 3. The expression of p-PERK and p-eIF2α proteins was analyzed by Western blot, and the protein concentrations were normalized to b-actin proteins levels (a and b). Data are expressed as the mean ± SEM of at least three independent experiments. $^{*}P < 0.05$, $^{**}P < 0.01$ versus vehicle-treated control; $^{\#}P < 0.05$, $^{\#\#}P < 0.01$ versus ox-LDL treatment; $^{\&}P < 0.05$, $^{\&\&}P < 0.01$ versus TM treatment. ox-LDL, oxidized LDL; p-PERK, phosphorylated protein kinase R like ER kinase; p-eIF2α, phosphorylated eukaryotic translation initiation factor 2α.

References

Bosma, M., Gerling, M., Pasto, J., et al., 2016. FNDC4 acts as an anti-inflammatory factor on macrophages and improves colitis in mice. Nat. Commun. 7, 11314.

Bostrom, P., Wu, J., Jedrychowski, M.P., et al., 2012. A PGC1-alpha-dependent myokine that drives brown-fat-like development of white fat and thermogenesis. Nature 481, 463–468.

Dun, S.L., Lyu, R.M., Chen, Y.H., Chang, J.K., Luo, J.J., Dun, N.J., 2013. Irisin-immunoreactivity in neural and non-neural cells of the rodent. Neuroscience 240, 155–162.

Feng, B., Yao, P.M., Li, Y., et al., 2003. The endoplasmic reticulum is the site of cholesterol-induced cytotoxicity in macrophages. Nat. Cell. Biol. 5, 781–792.

Finn, A.V., Nakano, M., Narula, J., Kolodgie, F.D., Virmani, R., 2010. Concept of vulnerable/unstable plaque. Arterioscler. Thromb. Vasc. Biol. 30, 1282–1292.

Fu, J., Han, Y., Wang, J., et al., 2016a. Irisin lowers blood pressure by improvement of endothelial dysfunction via AMPK-Akt-eNOS-NO pathway in the spontaneously hypertensive. Rat. J. Am. Heart Assoc. 5, pii: e003433.

Fu, J., Han, Y., Wang, J., Jose, P.A., Zeng, C., 2016b. Irisin lowered blood pressure by augmenting acetylcholine-mediated vasodilation via AMPK-Akt-eNOS-NO signal pathway in the spontaneously hypertensive. Rat. J. Am. Soc. Hypertens. 10 (Suppl 1), e4.

Kadoglou, N.P., Moustardas, P., Kapelouzou, A., et al., 2013. The anti-inflammatory effects of exercise training promote atherosclerotic plaque stabilization in apolipoprotein E knockout mice with diabetic atherosclerosis. Eur. J. Histochem. 57, e3.

Lu, J., Xiang, G., Liu, M., Mei, W., Xiang, L., Dong, J., 2015. Irisin protects against endothelial injury and ameliorates atherosclerosis in apolipoprotein E-Null diabetic mice. Atherosclerosis 243, 438–448.

Otsuka, F., Yasuda, S., Noguchi, T., Ishibashi-Ueda, H., 2016. Pathology of coronary atherosclerosis and thrombosis. Cardiovasc. Diagn. Ther. 6, 396–408.

Ron, D., Walter, P., 2007. Signal integration in the endoplasmic reticulum unfolded protein response. Nat. Rev. Mol. Cell Biol. 8, 519–529.

Rutkowski, D.T., Arnold, S.M., Miller, C.N., et al., 2006. Adaptation to ER stress is mediated by differential stabilities of pro-survival and pro-apoptotic mRNAs and proteins. PLoS Biol. 4, e374.

Scull, C.M., Tabas, I., 2011. Mechanisms of ER stress-induced apoptosis in atherosclerosis. Arterioscler. Thromb. Vasc. Biol. 31, 2792–2797.

Shimada, K., Mikami, Y., Murayama, T., et al., 2011. Atherosclerotic plaques induced by marble-burying behavior are stabilized by exercise training in experimental atherosclerosis. Int. J. Cardiol. 151, 284–289.

Song, H., Wu, F., Zhang, Y., et al., 2014. Irisin promotes human umbilical vein endothelial cell proliferation through the ERK signaling pathway and partly suppresses high glucose-induced apoptosis. PLoS One 9, e110273.

Tabas, I., 2010. The role of endoplasmic reticulum stress in the progression of atherosclerosis. Circ. Res. 107, 839–850.

Tabas, I., Ron, D., 2011. Integrating the mechanisms of apoptosis induced by endoplasmic reticulum stress. Nat. Cell. Biol. 13, 184–190.

Teufel, A., Malik, N., Mukhopadhyay, M., Westphal, H., 2002. Frcp1 and Frcp2, two novel fibronectin type III repeat containing genes. Gene 297, 79–83.

Thorp, E., Li, G., Seimon, T.A., Kuriakose, G., Ron, D., Tabas, I., 2009. Reduced apoptosis and plaque necrosis in advanced atherosclerotic lesions of Apoe-/- and Ldlr-/- mice lacking CHOP. Cell Metab. 9, 474–481.

Tsukano, H., Gotoh, T., Endo, M., et al., 2010. The endoplasmic reticulum stress-C/EBP homologous protein pathway-mediated apoptosis in macrophages contributes to the instability of atherosclerotic plaques. Arterioscler. Thromb. Vasc. Biol. 30, 1925–1932.

Wang, H., Zhao, Y.T., Zhang, S., et al., 2017. Irisin plays a pivotal role to protect the heart against ischemia and reperfusion injury. J. Cell. Physiol. http://dx.doi.org/10.1002/jcp.25857.

Wintergerst, E.S., Jelk, J., Rahner, C., Asmis, R., 2000. Apoptosis induced by oxidized low density lipoprotein in human monocyte-derived macrophages involves CD36 and activation of caspase-3. Eur. J. Biochem. 267, 6050–6059.

Wrann, C.D., White, J.P., Salogiannnis, J., et al., 2013. Exercise induces hippocampal BDNF through a PGC-1α/FNDC5 pathway. Cell. Metab. 18, 649–659.

Xiong, X.Q., Chen, D., Sun, H.J., et al., 2015. FNDC5 overexpression and irisin ameliorate glucose/lipid metabolic derangements and enhance lipolysis in obesity. Biochim. Biophys. Acta 1852, 1867–1875.

Yamazaki, H., Hiramatsu, N., Hayakawa, K., et al., 2009. Activation of the Akt-NF-kappaB pathway by subtilase cytotoxin through the ATF6 branch of the unfolded protein response. J. Immunol. 183, 1480–1487.

Yao, S., Zong, C., Zhang, Y., et al., 2013. Activating transcription factor 6 mediates oxidized LDL-induced cholesterol accumulation and apoptosis in macrophages by up-regulating CHOP expression. J. Atheroscler. Thromb. 20, 94–107.

Zhang, W., Chang, L., Zhang, C., et al., 2015. Central and peripheral irisin differentially regulate blood pressure. Cardiovasc. Drugs Ther. 29, 121–127.

Zhang, Y., Li, R., Meng, Y., et al., 2014. Irisin stimulates browning of white adipocytes through mitogen-activated protein kinase p38 MAP kinase and ERK MAP kinase signaling. Diabetes 63, 514–525.

Zhang, Y., Song, H., Wu, F., et al., 2016. Irisin inhibits atherosclerosis by promoting endothelial proliferation through microRNA126-5p. J. Am. Heart Assoc. 5, pii: e004031.

Zhu, G., Wang, J., Song, M., et al., 2016. Irisin increased the number and improved the function of endothelial progenitor cells in diabetes mellitus mice. J. Cardiovasc. Pharmacol. 68, 67–73.